The role of lipid composition in the antimicrobial peptide double cooperative effect

Yuge Hou, Kaori Sugihara*

Institute of Industrial Science, The University of Tokyo, 4-6-1 Komaba Meguro-Ku, Tokyo 153-8505, Japan

*Correspondence: kaori-s@iis.u-tokyo.ac.jp

ABSTRACT: The antimicrobial peptide double cooperative effect, where the mixture of two major antimicrobial peptides LL-37 and HNP1 kills bacteria more efficiently while minimizing the host damage by suppressing mammalian cell membrane lysis, has garnered attentions due to its potential applications towards efficient and safe antibiotics. However, its mechanism is completely unknown. In this work, we report that the double cooperative effect can be partially recapitulated in synthetic lipid systems just by varying the lipid composition between eukaryotic and *E. coli.* membranes. Although real cell membranes are so much more complex than just lipids, including *e.g.* membrane proteins and polysaccharides, our data implicates that one of the main driving forces of the double cooperative effect is a simple lipid-peptide interaction.

INTRODUCTION

Antimicrobial peptide (AMP) is one of the top candidates as an antibiotic alternative in the current crisis of the antibiotic resistance[1–7] because its mode of action that targets lipid membranes makes it difficult for bacteria to escape it via mutation.[8–17] To date seven AMP-based drugs are clinically in use as important last-resort treatments against resistant strains. However, many of them suffer from severe side effects such as hemolysis, nephrotoxicity and neurotoxicity,[18,19] being one of the bottlenecks for their broad applications.

Synergy or cooperative effect, where the mixture of different types of peptides presents enhanced antimicrobial efficiency,[20–25] has garnered attention as a strategy to overcome this bottleneck as increasing the potency enables lowering the dose. The most famous couple is PGLa and magainin-2, where the mechanism of their synergistic effect has been extensively studied by nuclear magnetic resonance (NMR), fluorescent leakage assay, circular dichroism (CD), and small-angle X-ray scattering (SAXS).[26–36] Another recent

example is LL-37 and HNP1. LL-37 is the only member of the human source cathelicidin family, which contains an amphiphilic α helical structure with the net charge +6.[37–46] It is known to destroy lipid bilayers via the carpet-like model,[40,41,43,44,47,48] in which LL-37 adheres on top of the lipid headgroups, aliens parallel to the bilayer, and disrupts the bilayer once a critical peptide-to-lipid ratio is reached,[49] which is the main mechanism of the antimicrobial effect.[50,51] Human neutrophile peptide 1 (HNP1) comes from the human defensin family, which consists of β-sheets connected with three disulfide bonds with the net charge +3.[52–58] It is produced in azurophil granules of neutrophiles, and often exists as dimers in solution that are connected by backbone-backbone hydrogen bonds.[52,59] Cell membrane permeation is the known antimicrobial mechanism, in which its tryptophan residue has a preference in binding to the lipid bilayer and the arginine residues are responsible for recognizing negatively charged bacterial membrane.[52,60–62] Nagaoka and the co-workers have reported that *Escherichia coli* (*E. coli*) and *Staphylococcus aureus* were killed more efficiently when LL-37 and HNP1 were combined.[63] In 2020, we have discovered that their mixture surprisingly supressed the cytotoxicity in eukaryotic cells,[64] where the inhibition of the LL-37 membrane destruction by HNP1 was the proposed mechanism. These reports together imply "the double cooperativity" between LL-37 and HNP1 that switches from membrane-destructive to membrane-protective functions, depending on whether the target is an enemy or a host. However, how these peptides switch their cooperative effect, depending on the target, is completely unknown.

In this work, biophysical techniques such as fluorescence recovery after photobleaching (FRAP), electrophysiology, tryptophan fluorescence assay, and CD are combined to investigate the mechanism of the double cooperative effect between LL-37 and HNP1. We will show that the double cooperative effect can be partially recapitulated in synthetic lipid systems just by varying the lipid composition between eukaryotic and *E. coli.* membranes. Although real cell membranes are so much more complex than just lipids, including e.g. membrane proteins and polysaccharides, our data implicates that one of the main driving forces of the double cooperative effect is a simple lipid-peptide interaction.

RESULTS AND DISCUSSIONS

FRAP indicates that changing the lipid composition from POPC to POPE/POPG/CL switches the LL-37-HNP1 cooperative effect from membrane-protective to membrane destructive. We hypothesized that the difference in the membrane composition between eukaryotic and bacterial cell membranes was the reason why the opposite functions were displayed when cells are incubated with the mixture of LL-37 and HNP1. In this work, as a first step, we will focus on the lipid composition difference. The first sign of the double cooperative effect was observed in fluorescence recovery after photobleaching (FRAP). FRAP is the standard method to monitor the lateral diffusion of lipids in cell membranes or supported lipid bilayers.[65–67] First, supported lipid bilayers[68,69] mimicking *E. coli* membrane composition[70] were formed on plasma-oxygen-activated glass coverslips by fusion of vesicles made of POPE/POPG/CL+1% NBD-PE in HEPES buffer solution with 2.0 mM Ca^{2+}. The composition of the lipids and its ratio were fixed based on that of natural *E. coli* lipid polar extracts and previous reports[71]. Ca^{2+} was used to eliminate the repulsion force between the negatively charged lipids (POPG and CL) and the glass as this method has been extensively studied before.[72] After rinsing the excess vesicles in the solution, a circular area was photobleached and the fluorescence recovery was monitored, from which the lipid diffusion coefficient and the mobile fraction were extracted (Figure 1a-c,

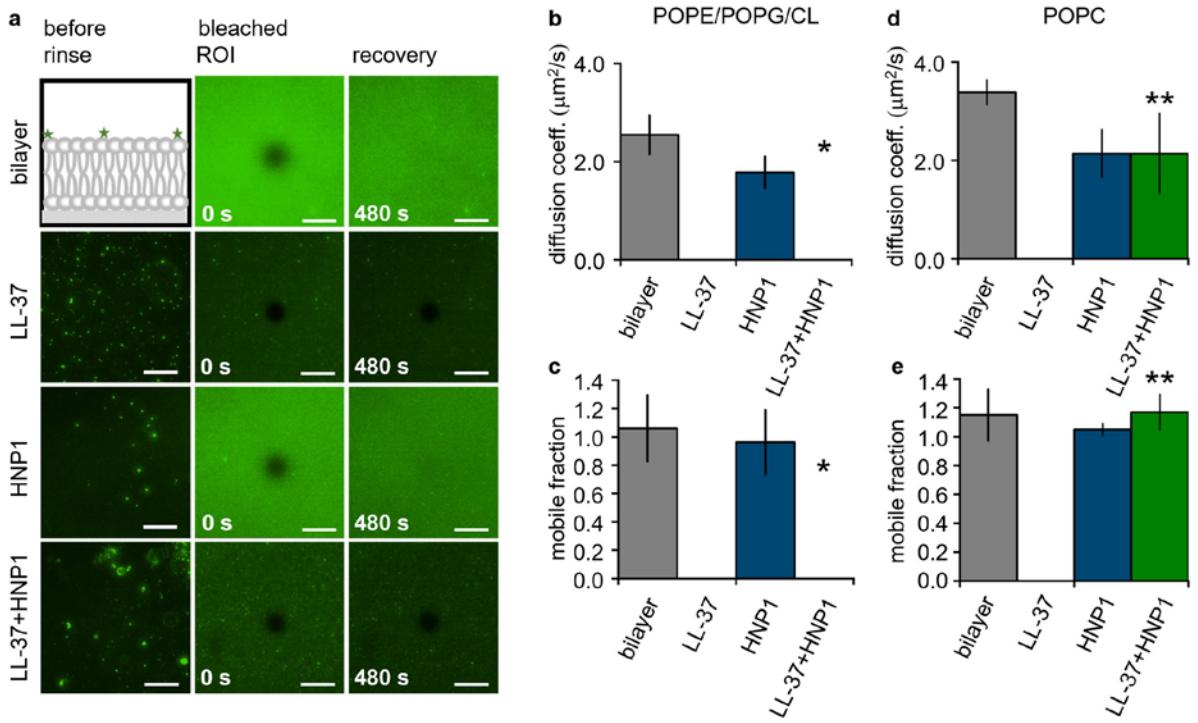

Figure 1: Fluorescence recovery after photobleaching (FRAP) results of supported POPE/POPG/CL lipid bilayers with 1% NBD-PE, incubated with 2.9 μM LL-37, HNP1 or their mixture (2.9 μM each). a, Fluorescence (stars in the upper left scheme represent the NBD from NBD-PE), **b,** extracted diffusion coefficient and **c,** the mobile fraction in POPE/POPG/CL system (n = 3). **d,** The diffusion coefficient and **e,** the mobile fraction in POPC bilayers (n = 3) have been adapted from ref [64] and presented with permission from Elsevier, copyright 2022. * and ** in b-e represent the LL-37 + HNP1 cooperative effect in POPC and POPE/POPG/CL. n represents the number of the experiments repeated to extract the average and the standard deviation (error bars) in the plots.

bilayer). The full recovery (mobile fraction of 1.06 ± 0.23) with a diffusion coefficient of D = 2.55 ± 0.40 μm^2/s is in agreement with the values in the literature.[73] LL-37 destroyed the lipid bilayers thus strongly disturbed the lateral diffusion, highlighted by the decreased fluorescence intensity, the diffusion coefficient D = 0.00 μm^2/s, and the mobile fraction = 0.00 (Figure 1a-c, LL-37). The effect of HNP1was minimum to the bilayer as FRAP almost fully recovered (mobile fraction 0.96 ± 0.23), although the diffusion coefficient was suppressed by 29.2% to D = 1.79 ± 0.32 μm^2/s, indicating that HNP1 inserted into the bilayer without rupturing it (Figure 1a-c, HNP1). The mixture of LL-37 + HNP1 demonstrated a significant loss in the fluorescence intensity, where the inhomogeneous bilayers with bright spots, the 0 diffusion coefficient, and the 0 mobile fraction suggest the destruction of the bilayers similar to the case of LL-37 (Figure 1a-c, LL-37 + HNP1. See *).

Previously, we have reported that a similar FRAP experiment against POPC supported lipid bilayers (eukaryotic cell membrane mimic) presented a completely different result, where mixing HNP1 rescued the LL-37 bilayer destruction. A part of those data are replotted in Figure 1d,e where both diffusion coefficient and the mobile fraction were elevated compared to the case of LL-37 (** in Figure 1d,e). These data together with the present work illustrate that the destruction of the bilayers by LL-37 is rescued by HNP1 in POPC membranes, whereas it does not in POPE/POPG/CL bilayers. This is the first indication that the cooperative effect between LL-37 and HNP1 are switching from membrane-protective (in POPC) to membrane-destructive (in POPE/POPG/CL), simply by altering the lipid composition.

Conductance measurements with pore-spanning bilayers also confirmed that the LL-37-HNP1 cooperative effect protects

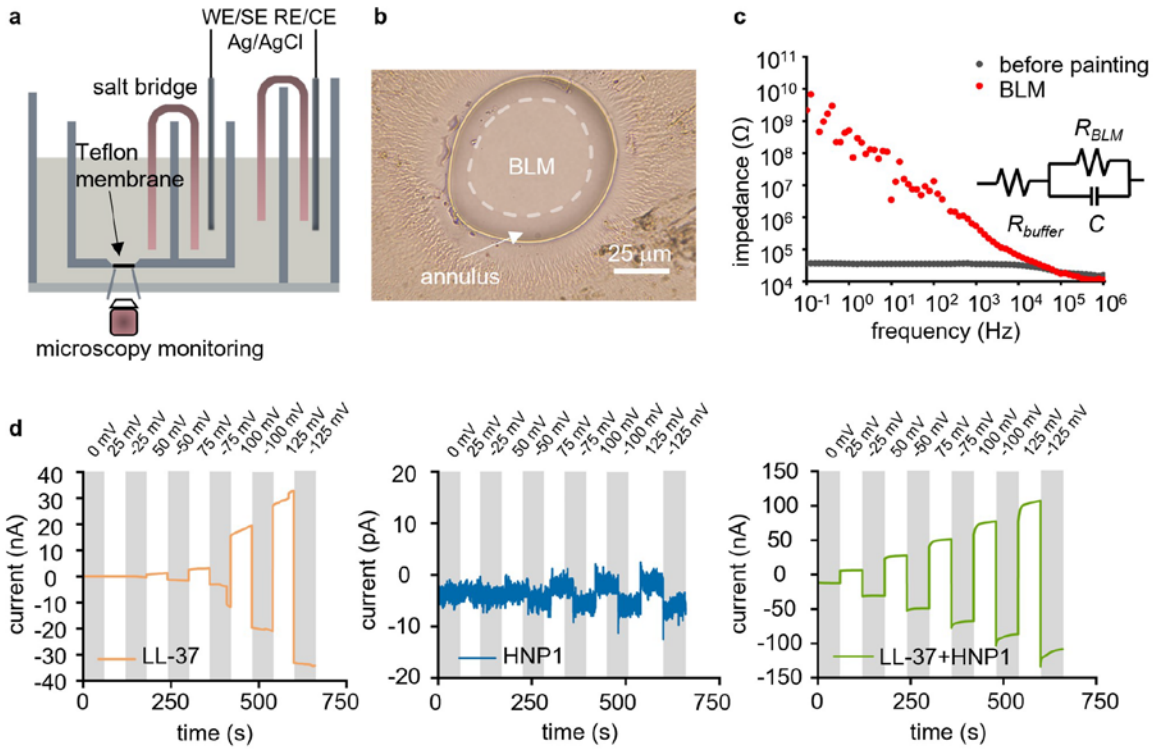

Figure 2: a, A schematic diagram of black lipid membrane (BLM) electrochemical chamber. **b,** A bright field image of a formed BLM. **c,** Impedance spectra of BLMs with the equivalent circuit used for fitting. **d,** Conductance measurements with BLMs after adding LL-37 (4.0 μM), HNP1 (2.0 μM) and the mixture of LL-37 + HNP1 (2.0 μM each) at 1:1 molar ratio.

POPC membranes, whereas destroys POPE/POPG/CL membranes. Next, to confirm the result from the FRAP, conductance measurements were performed with POPE/POPG/CL bilayers. Black lipid membrane (BLM) or pore-spanning membrane[74–76] is commonly used for studying ion channels or pore-forming peptides.[77–80] Recently, we have reported a lateral BLM setup (Figure 2a),[81] where the electrophysiological recording is coupled with an optical microscopy monitoring, which allows the bilayer thickness to be estimated more accurately compared to the conventional BLMs thanks to more precise reading of the BLM area (Figure 2b). POPE/POPG/CL in organic solvent was painted over the pore in a Teflon membrane at the bottom of the inner chamber under HEPES buffer solution (Figure 2a). With a help of the addition of bubbles for applying a pressure, thinning process took place and a BLM formed in the middle of the pore (Figure 2b). The impedance spectrum after painting was fitted with the equivalent circuit shown in Figure 2c, where the formed POPE/POPG/CL bilayer had a capacitance density of 0.47 μF/cm^2 that corresponds to the bilayer thickness of around 5.0 nm, which is consistent with the literature.[82] The average lifetime of this BLM was around 4 h, whereas all the presented data were obtained within the first 2 h to assure that the observed effect is from the peptides but not the instability of the BLMs. When LL-37 was added to the BLM, large defects formed, corresponding to the current at around 30 nA at 125 mV (Figure 2d), being in agreement with the carpet-like model that has been reported before.[41] When HNP1 was added to the bilayer, current at several pA was recorded, implying a minor defect formation (Figure 2d). When LL-37 and HNP1 were mixed, the membrane was also destroyed, evidenced by the current over 100 nA at 125 mV (Figure 2d). Although the recorded current for LL-37 + HNP1 (over 100 nA) was larger than the one for LL-37 (30 nA), this synergistic membrane destruction was difficult to confirm with the statistical significance, because the bilayer became so fragile with LL-37 or LL-37 + HNP1 that in

many cases it ruptured within several minutes once peptides were added. The result strongly contrasts our previously reported conductance measurements in POPC bilayers (eukaryotic membrane mimic), where the addition of HNP1 supressed the large current from LL-37 (the data shown in Figure S1).[64] The present data combined with our previous study in POPC bilayers indicate that HNP1 can rescue the membrane destruction by LL-37 in POPC, whereas it cannot or potentially even enhances it in POPE/POPG/CL bilayers. The result is consistent with that of FRAP. It is worth to note that the function of individual peptides (LL-37 or HNP1) did not have a significant lipid composition dependency, as qualitatively similar results were obtained both in POPC and POPE/POPG/CL. However, the concentration of the used peptides were 4.0 μM for LL-37, 2.0 μM for HNP1 and 2.0 μM each for the mixture in POPE/POPG/CL, whereas 8.0 μM for LL-37, 8.0 μM for HNP1 and 8.0 μM each for the mixture in POPC. This suggests that a smaller amount of peptides was required to generate the same function in POPE/POPG/CL membranes due to the electrostatic attraction between the lipid and the peptide (Figure S2) as we will discuss later.

LL-37 to HNP1 molar ratio can be elevated by more than an order of magnitude in a proximity to the POPE/POPG/CL membranes. Why did the lipid composition difference (POPC or POPE/POPG/CL) dramatically switch the function of LL-37 + HNP1 mixture, while the function of each peptide itself did not have a significant lipid dependency? To decipher this question, we test the following hypothesis.

Electrostatic forces between peptides and membranes are considered as a major element in the peptide-membrane interactions[83,84] and are commonly understood in the framework of the Gouy-Chapman theory.[85–87] In an ideal case, when a membrane has net charge zero (surface potential $\psi_0 = 0$), the concentration of LL-37 in the bulk and right above the membrane will be the same. However, when the membrane is negatively charged ($\psi_0 < 0$), LL-37 will be concentrated in proximity to the membrane due to the electrostatic attraction. This peptide concentration close to the membrane (in the electrical double layer characterized by the Debye length ~ 0.785 nm at 150 mM NaCl) can be roughly estimated from the following (eq. 1):[85]

$$C_s = C_b e^{-zF_0\psi_0/RT}, \qquad \text{(eq. 1)}$$

where C_s and C_b are the peptide concentration right above the membrane and in the bulk solution, respectively, z is the net charge of the peptide, F_0 is the Faraday constant, ψ_0 is the surface potential of the membrane, R is the gas constant and T is the temperature. Now, we will discuss different scenarios, keeping our mind that POPG and CL are negatively charged,[88–90] whereas POPE and POPC are zwitterionic (Figure 3a). When LL-37 (net charge z = +6) was added to POPE/POPG/CL membranes, C_s can be calculated as $C_s = 2.64 \times 10^3\, C_b$, where F_0 = 9.65 × 10^4 C mo1^{-1}, R = 8.31 J K^{-1} mol^{-1}, T = 298 K, and ψ_0 = -33.7 mV based on zeta potential measurements (Table S1). Although this value is not quantitively precise as we used zeta potential instead of surface potential and as the effective charge of LL-37 is less than +6 due to the ion screening, LL-37 can be potentially concentrated over a thousand folds right above the anionic membrane, as similar effects have been discussed before.[91] Now, we consider the addition of HNP1, which has a net charge z = +3. When we add HNP1 and LL-37 at 1:1 molar ratio in the bulk, around POPC membrane (supposing $\psi_0 = 0$), this ratio is maintained. However, around POPE/POPG/CL membranes, surprisingly, the ratio could be twisted as bad as 1:51, calculated from (eq. 1), just because the electric charges of the peptides are different (Figure 3b). It implies that as far as the

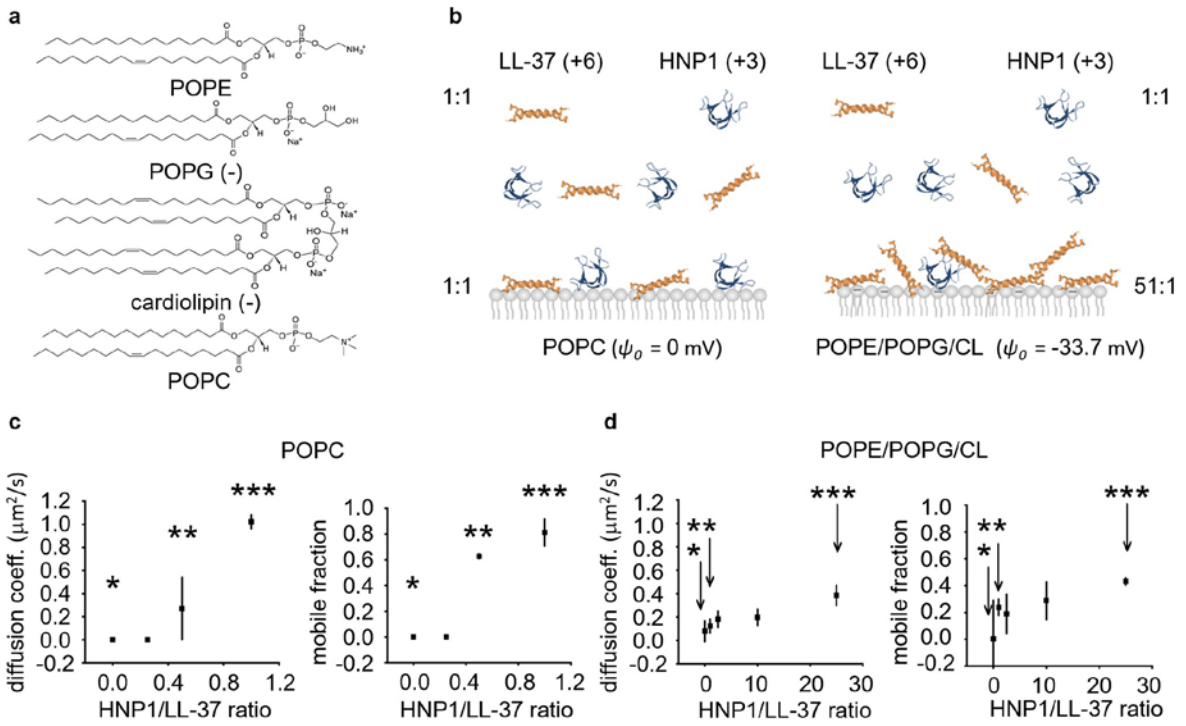

Figure 3: a, The chemical structure of POPE, POPG, CL, and POPC**. b,** Schemes showing the concentration of cationic peptides close to anionic bilayers based on Gouy-Chapman theory. The diffusion coefficient and the mobile fraction of **c,** POPC bilayer and **d,** POPE/POPG/CL bilayer as a function of HNP1/LL-37 molar ratio (n = 3, LL-37 was always kept at 5.8 μM).

membranes are concerned the presence of HNP1 is almost negligible compared to the over-crowded LL-37, despite the fact that we added the same amount of LL-37 and HNP1 in the solution. This could explain the lack of the neutralization of the LL-37 membrane destruction by HNP1 in POPE/POPG/CL as simply such an extreme small fraction of HNP1 compared to LL-37 was not enough to present any cooperative effect.

The cooperative effect depends on the LL-37 to HNP1 molar ratio. To test this hypothesis, we performed a simple FRAP experiment, where the molar ratio of LL-37 and HNP1 were varied in POPC and POPE/POPG/CL supported lipid bilayers. First, for POPC, addition of only LL-37 at 5.8 μM completely destroyed the bilayer, confirmed by D = 0.00 μm^2/s and the mobile fraction = 0.00 (* in Figure 3c), which is consistent with our previous report.[92] When HNP1 was mixed at HNP1/LL-37 = 0.5, the diffusion coefficient and the mobile fraction increased to 0.27 ± 0.27 μm^2/s and 0.63 ± 0.01, respectively (** in Figure 3c), yet the mobile fraction reached 0.81 ± 0.11 only at HNP1/LL-37 = 1 with D = 1.02 ± 0.06 μm^2/s (*** in Figure 3c). This suggests that the cooperative effect is molar ratio dependent and needs around 1:1 molar ratio to be efficiently displayed. For POPE/POPG/CL, addition of LL-37 at 5.8 μM destroyed the bilayers as evidenced by D = 0.08 ± 0.09 μm^2/s and the mobile fraction = 0.20 ± 0.29 (* in Figure 3d). Mixing HNP1 at 1:1 bulk ratio could not neutralize it (D = 0.12 ± 0.06 μm^2/s and the mobile fraction = 0.44 ± 0.06 shown with ** in Figure 3d), as also shown in Figure 1a-c. However, increasing the HNP1/LL-37 bulk ratio further up to 25 elevated the diffusion coefficient and the mobile fraction to D = 0.39 ± 0.09 μm^2/s and 0.63 ± 0.03, respectively (*** in Figure 3d), This indicates that HNP1 can also partially rescue the LL-37 bilayer destruction in POPE/POPG/CL membranes as long as enough amount is added. The result supports that the HNP1/LL-37 molar ratio is the key factor to exhibit the cooperative effect.

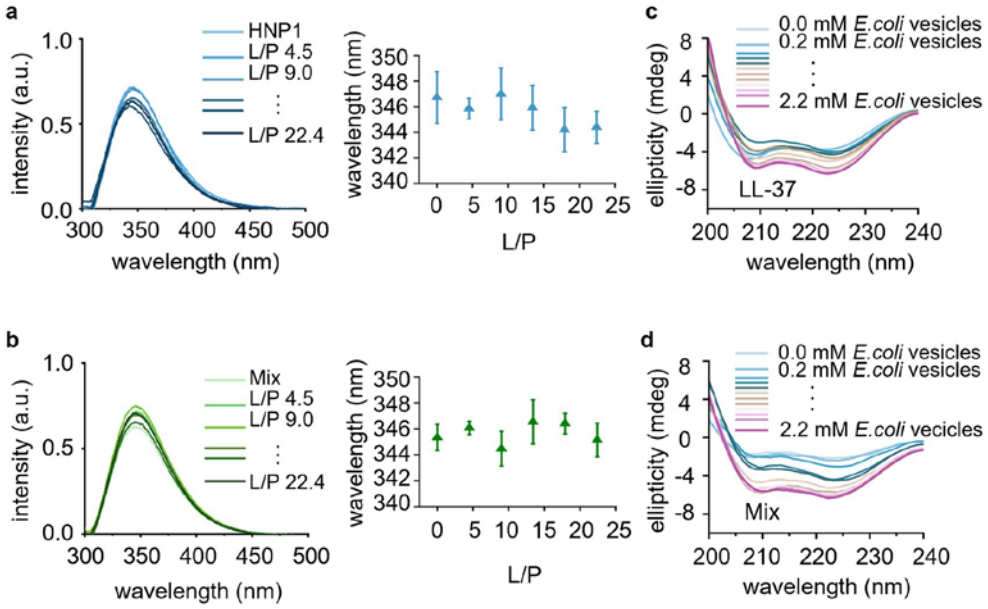

Figure 4: Tryptophan (Trp) fluorescence results, fluorescence emission spectrum, peak shift of a, HNP1 (2.9 μM) and **b,** mixture of LL-37 + HNP1 (per 2.9 μM) with titration of POPE/POPG/CL vesicles solution resulting in deferent lipid/peptide (L/P) ratios (n = 3, LL-37 spectra was subtracted). CD spectra of **c,** LL-37 and **d,** the mixture of LL-37 + HNP1 with titration of 15.0 mM POPE/POPG/CL vesicle suspension at 2.0 μL every 5 min, at peptide concentration of (per) 29.0 μM, with a final lipid concentration at 2.2 mM (HNP1 spectra was subtracted). All experiments were done in HEPES buffer solution (10 mM HEPES, 150 mM NaCl, pH = 7.4).

Therefore, together with the Gouy-Chapman theory, it supports our hypothesis that the absence of the cooperative effect in the anionic POPE/POPG/CL membranes was because the HNP1/LL-37 ratio at the membrane was not high enough when they are added at 1:1 ratio in the bulk solution. This effect occurred also in other anionic membranes regardless of the lipid composition (Figure S3, 4). Note that although we assumed the monomeric charges for estimating the HNP1/LL-37 ratio right above the membranes, their oligomeric state will affect the net charges, and thus the ratio in the reality. Previously, PGLa and magainin-2 have been also found to present a synergistic effect in a molar-ratio-dependent manner.[93–95]

Tryptophan fluorescence assay and CD suggest that LL-37 slightly suppresses the penetration of HNP1 into POPE/POPG/CL bilayers, whereas the structure of LL-37 was not affected by HNP1. The discussion in the previous paragraph led to the conclusion that the presence of HNP1 was almost negligible in POPE/POPG/CL membranes when LL-37 and HNP1 were added at 1:1 bulk ratio. To test whether HNP1 truly had no effect on the membrane, we studied the structure of the peptide-lipid complex by tryptophan fluorescence assay and CD. In physiological buffer solution, both LL-37 and HNP1 are known to form oligomers at the micromolar concentration range used in this work.[49,96] In negatively-charged bilayers, both monomeric[49] and oligomeric states[97] were suggested for LL-37 in the framework of the carpet-like model, whereas HNP1 is typically found as a dimeric pore. HNP1 contains one tryptophan residue. In the hydrophobic environment tryptophan emission causes a blue shift[98–102] which can be used to probe its local environment. When HNP1 is incubated with POPE/POPG/CL small unilamellar vesicles (SUV), it slightly goes into the bilayers, evidenced by a subtle blue shift (Figure 4a). Previously, we have reported similar data for HNP1 in POPC

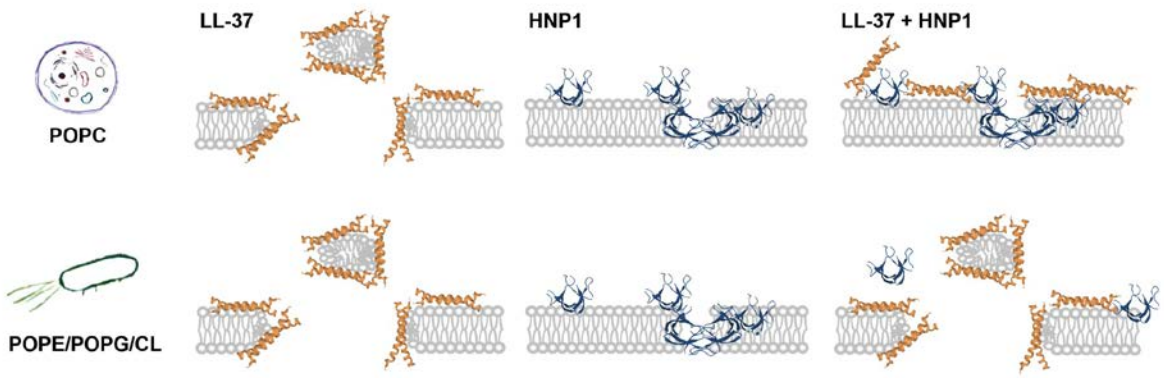

Figure 5: A scheme showing a possible model for the mechanism of LL-37, HNP1 and LL-37 + HNP1 functions in POPC and POPE/POPG/CL lipid bilayers.

reported similar data for HNP1 in POPC vesicles.[64] When HNP1 + LL-37 mixture at 1:1 was incubated with the vesicles, no obvious peak shift was observed (Figure 4b), implying that the over-crowded LL-37 at the membranes, which originated from the charge difference between LL-37 and HNP1, hindered HNP1 to penetrate the bilayers.

Next, CD was performed for the characterization of the peptide secondary structure. LL-37 adopted a helical structure already in the buffer solution, highlighted by the characteristic double dip at 208 nm and 222 nm for α helix (Figure 4c),[103,104] as it has already been reported before.[47,105] The titration with POPE/POPG/CL vesicles strengthened the double dip as the hydrophobic environment enhanced the helical structure. When the LL-37 + HNP1 mixture was titrated with the vesicles, a similar result was obtained (Figure 4c). This indicates that HNP1 did not significantly affect the α helical structure of LL-37 and neither did LL-37 alter the structure of HNP1 in the vesicles. These two experiments suggest that LL-37 seems to be slightly suppressing the penetration of HNP1, whereas the structure of LL-37 was not affected by HNP1, which is consistent with our hypothesis.

CONCLUSION

We reported that the cooperative function between LL-37 and HNP1 switches between membrane-protective to membrane-destructive just by varying the lipid composition between eukaryotic (POPC) and *E. coli.* membranes (POPE/POPG/CL) (Figure 5). This was rationalized by a model based on the modulation of the LL-37 to HNP1 molar ratio right above the membranes. When the membrane is electrically neutral (POPC), 1:1 molar ratio of the added peptides in the bulk solution is maintained in the proximity to the membrane. This generated the cooperative effect, where the LL-37 membrane destruction was neutralized by HNP1. However, when the membrane is negatively charged (POPE/POPG/CL), the theory predicts that the molar ratio close to the membrane can be even as bad as LL-37/HNP1 = 51, just because their electric charges are different (+6 for LL-37 and +3 for HNP1). This explains the lack of cooperative effect in POPE/POPG/CL, simply because the amount of HNP1 was not enough. Consequently, only the function of LL-37 was predominantly displayed, resulting in the membrane destruction. This model explains the switch between the membrane-protective to membrane-destructive functions via the presence or the absence of the neutralization of LL-37 membrane destruction by HNP1. Therefore, it does not provide a reason for the synergy observed in the bacterial assay *in-vitro*,[63] where the mixture of LL-37 and HNP1 "enhanced" the antimicrobial efficiency. This suggests that although the lipid-peptide electrostatic interactions can partially rationalize the phenomenon, other membrane components

such as membrane proteins and polysaccharides or other effects such as peptide-peptide interactions in membranes and the effect of the inner- and outer-membrane structure in gram-negative bacteria have to be taken into account to fully explain the double cooperative effect.

SUPPLEMENTARY INFORMATION

Materials and methods, supporting figures for results of black lipid membranes (BLM) in POPC membranes (Figure S1-S2), results of fluorescence recovery after photobleaching (FRAP) in different lipid membrane systems (Figure S3-S4), and a supporting table for zeta potential results (Table S1) are presented in the Supplementary information.

ACKNOWLEDGEMENTS

Part of the research leading to these results has received funding from UTEC-UTokyo FSI Research Grant Program, the FY 2020 University of Tokyo Excellent Young Researcher, Takeda Science Foundation, Mitsubishi Foundation, Inoue Foundation for Science, Naito Foundation, Fuji Seal Foundation, JSPS KAKENHI Grant Number JP22K03544, JP22H04525, JST FOREST Program Grant Number JPMJFR211Q, and JPNP20004, subsidized by the New Energy and Industrial Technology Development Organization (NEDO). We thank Prof. Kazuaki Kudo (IIS, Univ. Tokyo) for the instrumental access to CD, Prof. Tetsu Tatsuma (IIS, Univ. Tokyo) for the fluorescent spectrometer and Prof. Tsuyoshi Minami (IIS, Univ. Tokyo) for the Zeta-potential analyzer.

REFERENCES

(1) Michael, C. A.; Dominey-Howes, D.; Labbate, M. The Antimicrobial Resistance Crisis: Causes, Consequences, and Management. *Front. Public Health* **2014**, 2,145

(2) Chandler, C. I. R. Current Accounts of Antimicrobial Resistance: Stabilisation, Individualisation and Antibiotics as Infrastructure. *Palgrave Communications* **2019**, *5* (1).

(3) Prestinaci, F.; Pezzotti, P.; Pantosti, A. Antimicrobial Resistance: A Global Multifaceted Phenomenon. *Pathog. Glob. Health* **2015**, *109* (7), 309–318.

(4) Murray, C. J.; Ikuta, K. S.; Sharara, F.; Swetschinski, L.; Robles Aguilar, G.; Gray, A.; Han, C.; Bisignano, C.; Rao, P.; Wool, E.; Johnson, S. C.; Browne, A. J.; Chipeta, M. G.; Fell, F.; Hackett, S.; Haines-Woodhouse, G.; Kashef Hamadani, B. H.; Kumaran, E. A. P.; McManigal, B.; Agarwal, R.; Akech, S.; Albertson, S.; Amuasi, J.; Andrews, J.; Aravkin, A.; Ashley, E.; Bailey, F.; Baker, S.; Basnyat, B.; Bekker, A.; Bender, R.; Bethou, A.; Bielicki, J.; Boonkasidecha, S.; Bukosia, J.; Carvalheiro, C.; Castañeda-Orjuela, C.; Chansamouth, V.; Chaurasia, S.; Chiurchiù, S.; Chowdhury, F.; Cook, A. J.; Cooper, B.; Cressey, T. R.; Criollo-Mora, E.; Cunningham, M.; Darboe, S.; Day, N. P. J.; de Luca, M.; Dokova, K.; Dramowski, A.; Dunachie, S. J.; Eckmanns, T.; Eibach, D.; Emami, A.; Feasey, N.; Fisher-Pearson, N.; Forrest, K.; Garrett, D.; Gastmeier, P.; Giref, A. Z.; Greer, R. C.; Gupta, V.; Haller, S.; Haselbeck, A.; Hay, S. I.; Holm, M.; Hopkins, S.; Iregbu, K. C.; Jacobs, J.; Jarovsky, D.; Javanmardi, F.; Khorana, M.; Kissoon, N.; Kobeissi, E.; Kostyanev, T.; Krapp, F.; Krumkamp, R.; Kumar, A.; Kyu, H. H.; Lim, C.; Limmathurotsakul, D.; Loftus, M. J.; Lunn, M.; Ma, J.; Mturi, N.; Munera-Huertas, T.; Musicha, P.; Mussi-Pinhata, M. M.; Nakamura, T.; Nanavati, R.; Nangia, S.; Newton, P.; Ngoun, C.; Novotney, A.; Nwakanma, D.; Obiero, C. W.; Olivas-Martinez, A.; Olliaro, P.; Ooko, E.; Ortiz-Brizuela, E.; Peleg, A. Y.; Perrone, C.; Plakkal, N.; Ponce-de-Leon, A.; Raad, M.; Ramdin, T.; Riddell, A.; Roberts, T.; Robotham, J. V.; Roca, A.; Rudd, K. E.; Russell, N.; Schnall, J.; Scott, J. A. G.; Shivamallappa, M.; Sifuentes-Osornio, J.; Steenkeste, N.; Stewardson, A. J.; Stoeva, T.; Tasak, N.; Thaiprakong, A.; Thwaites, G.; Turner, C.; Turner, P.; van Doorn, H. R.; Velaphi, S.; Vongpradith, A.; Vu, H.; Walsh, T.; Waner, S.; Wangrangsimakul, T.; Wozniak, T.; Zheng, P.; Sartorius, B.; Lopez, A. D.; Stergachis, A.; Moore, C.; Dolecek, C.; Naghavi, M. Global Burden of Bacterial Antimicrobial Resistance in 2019: A Systematic Analysis. *The Lancet* **2022**, *399* (10325), 629–655.

(5) https://www.cdc.gov/drugresistance/covid19.html, 2023, 5, 5.

(6) Knight, G. M.; Glover, R. E.; McQuaid, C. F.; Olaru, I. D.; Gallandat, K.; Leclerc, Q. J.; Fuller, N. M.; Willcocks, S. J.; Hasan, R.; van Kleef, E.; Chandler, C. I. R. Antimicrobial Resistance and Covid-19: Intersections and Implications. *eLife* **2021**, 10, 1–27.

(7) Koivuniemi A.; Fallarero A.; Bunker A.. Insight into the antimicrobial mechanism of action of β2, 2-amino acid derivatives from molecular dynamics simulation: Dancing the can-can at the membrane surface. *BBA-Biomembranes* **2019**, *1861* (11), 183028.

(8) Le, C. F.; Fang, C. M.; Sekaran, S. D. Intracellular Targeting Mechanisms by Antimicrobial Peptides. *Antimicrob. Agents Ch.* **2017**, *61* (4), e02340-16.

(9) Zhang, L. J.; Gallo, R. L. Antimicrobial peptides. *Curr. Biol.* **2016**, *26* (1), 14-19.

(10) Erdem Büyükkiraz, M.; Kesmen, Z. Antimicrobial Peptides (AMPs): A Promising Class of Antimicrobial Compounds. *J. Appl. Microbiol.* **2022**, *132* (3), 1573-1596.

(11) Lazzaro, B. P.; Zasloff, M.; Rolff, J. Antimicrobial Peptides: Application Informed by Evolution. *Science* **2020**, *368* (6490), 5480.

(12) Moravej, H.; Moravej, Z.; Yazdanparast, M.; Heiat, M.; Mirhosseini, A.; Moosazadeh Moghaddam, M.; Mirnejad, R. Antimicrobial Peptides: Features, Action, and Their Resistance Mechanisms in Bacteria. *Microb. Drug Resist.* **2018**, *24* (6), 747–767.

(13) Gan, B. H.; Gaynord, J.; Rowe, S. M.; Deingruber, T.; Spring, D. R. The Multifaceted Nature of Antimicrobial Peptides: Current Synthetic Chemistry Approaches and Future Directions. *Chem. Soc. Rev.* **2021**, *50* (13), 7820-7880.

(14) Lei, J.; Sun, L.; Huang, S.; Zhu, C.; Li, P.; He, J.; Mackey, V.; Coy, D. H.; He, Q. The Antimicrobial Peptides and Their Potential Clinical Applications; *Am. J. Transl. Res.* **2019**, *11* (7), 3919-3931.

(15) Mahlapuu, M.; Håkansson, J.; Ringstad, L.; Björn, C. Antimicrobial Peptides: An Emerging Category of Therapeutic Agents. *Front. Cell. Infect. Mi.* **2016**, 194.

(16) Huan, Y.; Kong, Q.; Mou, H.; Yi, H. Antimicrobial Peptides: Classification, Design, Application and Research Progress in Multiple Fields. *Front. Microbiol.* **2020**, 2559.

(17) Moretta, A.; Scieuzo, C.; Petrone, A. M.; Salvia, R.; Manniello, M. D.; Franco, A.; Lucchetti, D.; Vassallo, A.; Vogel, H.; Sgambato, A.; Falabella, P. Antimicrobial Peptides: A New Hope in Biomedical and Pharmaceutical Fields. *Front. Cell. Infect. Mi.* **2021**, 453.

(18) Rai, A.; Ferrão, R.; Palma, P.; Patricio, T.; Parreira, P.; Anes, E.; Tonda-Turo, C.; Martins, M. C. L.; Alves, N.; Ferreira, L. Antimicrobial Peptide-Based Materials: Opportunities and Challenges. *J. Mater. Chem. B* **2022**, 2384–2429.

(19) Gou, S.; Li, B.; Ouyang, X.; Ba, Z.; Zhong, C.; Zhang, T.; Chang, L.; Zhu, Y.; Zhang, J.; Zhu, N.; Zhang, Y.; Liu, H.; Ni, J. Novel Broad-Spectrum Antimicrobial Peptide Derived from Anoplin and Its Activity on Bacterial Pneumonia in Mice. *J. Med. Chem.* **2021**, *64* (15), 11247–11266.

(20) Han, E.; Lee, H. Synergistic Effects of Magainin 2 and PGLa on Their Heterodimer Formation, Aggregation, and Insertion into the Bilayer. *RSC Adv.* **2015**, *5* (3), 2047–2055.

(21) Marquette, A.; Salnikov, E. S.; Glattard, E.; Aisenbrey, C.; Bechinger, B. Magainin 2-PGLa Interactions in Membranes-Two Peptides That Exhibit Synergistic Enhancement of Antimicrobial Activity. *Curr. Top. Med. Chem.* **2016**, 16.

(22) Aisenbrey, C.; Amaro, M.; Pospíšil, P.; Hof, M.; Bechinger, B. Highly Synergistic Antimicrobial Activity of Magainin 2 and PGLa Peptides Is Rooted in the Formation of Supramolecular Complexes with Lipids. *Sci. Rep.* **2020**, *10* (1).

(23) Westerhoff, H. v.; Zasloff, M.; Rosner, J. L.; Hendler, R. W.; Waal, A.; Gomes, A. V.; Jongsma, A. P. M.; Riethorst, A.; Juretic, D. Functional Synergism of the Magainins PGLa and Magainin-2 in Escherichia Coli, Tumor Cells and Liposomes. *Eur. J. Biochem.* **1995**, *228* (2), 257–264.

(24) Yan, H.; Hancock, R. E. W. Synergistic Interactions between Mammalian Antimicrobial Defense Peptides. *Antimicrob. Agents Ch.* **2001**, *45* (5), 1558–1560.

(25) Matsuzaki, K.; Mitani, Y.; Akada, K. Y.; Murase, O.; Yoneyama, S.; Zasloff, M.; Miyajima, K. Mechanism of Synergism between Antimicrobial Peptides Magainin 2 and PGLa. *Biochemistry* **1998**, *37* (43), 15144–15153.

(26) Zerweck, J.; Strandberg, E.; Bürck, J.; Reichert, J.; Wadhwani, P.; Kukharenko, O.; Ulrich, A. S. Homo- and Heteromeric Interaction Strengths of the Synergistic Antimicrobial Peptides PGLa and Magainin 2 in Membranes. *Eur. Biophys. J.* **2016**, *45* (6), 535–547.

(27) Zerweck, J.; Strandberg, E.; Kukharenko, O.; Reichert, J.; Bürck, J.; Wadhwani, P.; Ulrich, A. S. Molecular Mechanism of Synergy between the Antimicrobial Peptides PGLa and Magainin 2. *Sci. Rep.* **2017**, *7* (1).

(28) Strandberg, E. , Tremouilhac, P. , Wadhwani, P. , Ulrich, A. S.;Synergistic Transmembrane Insertion of the Heterodimeric PGLa/magainin 2 Complex Studied by Solid-State NMR. *BBA-Biomembranes* **1788** (8), 1667-1679.

(29) Pachler, M.; Kabelka, I.; Appavou, M. S.; Lohner, K.; Vácha, R.; Pabst, G. Magainin 2 and PGLa in Bacterial Membrane Mimics I: Peptide-Peptide and Lipid-Peptide Interactions. *Biophys. J.* **2019**, *117* (10), 1858–1869.

(30) Kabelka, I.; Pachler, M.; Prévost, S.; Letofsky-Papst, I.; Lohner, K.; Pabst, G.; Vácha, R. Magainin 2 and PGLa in Bacterial Membrane Mimics II: Membrane Fusion and Sponge Phase Formation. *Biophys. J.* **2020**, *118* (3), 612–623.

(31) Kabelka, I.; Georgiev, V.; Marx, L.; Pajtinka, P.; Lohner, K.; Pabst, G.; Dimova, R.; Vácha, R. Magainin 2 and PGLa in Bacterial Membrane Mimics III: Membrane Fusion and Disruption. *Biophys. J.* **2022**, *121* (5), 852–861.

(32) Ma, W.; Sun, S.; Li, W.; Zhang, Z.; Lin, Z.; Xia, Y.; Yuan, B.; Yang, K. Individual Roles of Peptides PGLa and Magainin 2 in Synergistic Membrane Poration. *Langmuir* **2020**, *36* (26), 7190–7199.

(33) Aisenbrey, C.; Amaro, M.; Pospíšil, P.; Hof, M.; Bechinger, B. Highly Synergistic Antimicrobial Activity of Magainin 2 and PGLa Peptides Is Rooted in the Formation of Supramolecular Complexes with Lipids. *Sci. Rep.* **2020**, *10* (1).

(34) Juhl, D. W.; Glattard, E.; Lointier, M.; Bampilis, P.; Bechinger, B. The Reversible Non-Covalent Aggregation into Fibers of PGLa and Magainin 2 Preserves Their Antimicrobial Activity and Synergism. *Front. Cell. Infect. Microbiol.* **2020**, *10*.

(35) Bechinger, B.; Juhl, D. W.; Glattard, E.; Aisenbrey, C. Revealing the Mechanisms of Synergistic Action of Two Magainin Antimicrobial Peptides. *Front. Med. Technol.* **2020**, *2*.

(36) Glattard, E.; Salnikov, E. S.; Aisenbrey, C.; Bechinger, B. Investigations of the Synergistic Enhancement of Antimicrobial Activity in Mixtures of Magainin 2 and PGLa. *Biophys. Chem.* **2016**, *210*, 35–44.

(37) Sochacki, K. A.; Barns, K. J.; Bucki, R.; Weisshaar, J. C. Real-Time Attack on Single Escherichia Coli Cells by the Human Antimicrobial Peptide LL-37. *Proc. Natl. Acad. Sci. USA* **2011**, *108* (16), 77-81.

(38) Scheenstra, M, R.; Matthias, V, D, B.; Tjeerdsma-Van B.; Johanna, L, M.; Schneider, Viktoria, A, F.; Ordonez; Soledad, R.; van, D.; Albert; Veldhuizen; Edwin, J, A.; Haagsman; Henk, P. Cathelicidins PMAP-36, LL-37 and CATH-2 are similar peptides with different modes of action. *Sci. Rep.* **2019**, *9* (1).

(39) Zhu, Y.; Mohapatra, S.; Weisshaar, J. C. Rigidification of the Escherichia Coli Cytoplasm by the Human Antimicrobial Peptide LL-37 Revealed by Superresolution Fluorescence Microscopy. *Proc. Natl. Acad. Sci. USA* **2019**, *116* (3), 1017–1026.

(40) Lee, C. C.; Sun, Y.; Qian, S.; Huang, H. W. Transmembrane Pores Formed by Human Antimicrobial Peptide LL-37. *Biophys. J.* **2011**, *100* (7), 1688–1696.

(41) Sancho-Vaello, E.; Gil-Carton, D.; François, P.; Bonetti, E. J.; Kreir, M.; Pothula, K. R.; Kleinekathöfer, U.; Zeth, K. The Structure of the Antimicrobial Human Cathelicidin LL-37 Shows Oligomerization and Channel Formation in the Presence of Membrane Mimics. *Sci. Rep.* **2020**, *10* (1).

(42) Wang, G.; Mishra, B.; Epand, R. F.; Epand, R. M. High-Quality 3D Structures Shine Light on Antibacterial, Anti-Biofilm and Antiviral Activities of Human Cathelicidin LL-37 and Its Fragments. *BBA-Biomembranes* **2014**, 2160–2172.

(43) Henzler Wildman, K. A.; Lee, D. K.; Ramamoorthy, A. Mechanism of Lipid Bilayer Disruption by the Human Antimicrobial Peptide, LL-37. *Biochemistry* **2003**, *42* (21), 6545–6558.

(44) Thennarasu, S.; Tan, A.; Penumatchu, R.; Shelburne, C. E.; Heyl, D. L.; Ramamoorthy, A. Antimicrobial and Membrane Disrupting Activities of a Peptide Derived from the Human Cathelicidin Antimicrobial Peptide Ll37. *Biophys. J.* **2010**, *98* (2), 248–257.

(45) Gambade, A.; Zreika, S.; Guéguinou, M.; Chourpa, I.; Fromont, G.; Bouchet, A. M.; Burlaud-Gaillard, J.; Potier-Cartereau, M.; Roger, S.; Aucagne, V.; Chevalier, S.; Vandier, C.; Goupille, C.; Weber, G. Activation of TRPV2 and BKCa Channels by the LL-37 Enantiomers Stimulates Calcium Entry and Migration of Cancer Cells. *Oncotarget* **2016,** *7* (17):23785-23800**.**

(46) Johansson, J.; Gudmundsson, G. H.; Rottenberg, M. E.; Berndt, K. D.; Agerberth, B. Conformation-Dependent Antibacterial Activity of the Naturally Occurring Human Peptide LL-37 *J. Biol. Chem.* **1998**, *273* (6):3718-3724.

(47) Xhindoli, D.; Pacor, S.; Benincasa, M.; Scocchi, M.; Gennaro, R.; Tossi, A. The Human Cathelicidin LL-37 - A Pore-Forming Antibacterial Peptide and Host-Cell Modulator. *Biochim. Biophys. Acta. Biomembr.* **2016**, *1858* (3), 546–566.

(48) Sevcsik, E.; Pabst, G.; Richter, W.; Danner, S.; Amenitsch, H.; Lohner, K. Interaction of LL-37 with Model Membrane Systems of Different Complexity: Influence of the Lipid Matrix. *Biophys. J.* **2008**, *94* (12), 4688–4699.

(49) Oren, Z.; Lerman, J. C.; Gudmundsson, G. H.; Agerberth, B.; Shai, Y. Structure and Organization of the Human Antimicrobial Peptide LL-37 in Phospholipid Membranes. *Biochem. J.* **1999**, *341* (3), 501-513.

(50) Sancho-Vaello, E.; Gil-Carton, D.; François, P.; Bonetti, E. J.; Kreir, M.; Pothula, K. R.; Kleinekathöfer, U.; Zeth, K. The Structure of the Antimicrobial Human Cathelicidin LL-37 Shows Oligomerization and Channel Formation in the Presence of Membrane Mimics. *Sci. Rep.* **2020**, *10* (1).

(51) Sochacki, K. A.; Barns, K. J.; Bucki, R.; Weisshaar, J. C. Real-Time Attack on Single Escherichia Coli Cells by the Human Antimicrobial Peptide LL-37. *Proc. Natl. Acad. Sci. USA* **2011**, *108* (16).

(52) Pazgier, M.; Wei, G.; Ericksen, B.; Jung, G.; Wu, Z.; de Leeuw, E.; Yuan, W.; Szmacinski, H.; Lu, W. Y.; Lubkowski, J.; Lehrer, R. I.; Lu, W. Sometimes It Takes Two to Tango: Contributions of Dimerization to Functions of Human α-Defensin HNP1 Peptide. *J. Biol. Chem.* **2012**, *287* (12), 8944–8953.

(53) Lehrer,R,I.; Lu,W. α-Defensins in human innate immunity. *Immunol. Rev.* **2012**, *245* (1):84-112.

(54) Kagan, B. L.; Selsted, M. E.; Ganz, T.; Lehrer, R.; Angeles, L. Antimicrobial Defensin Peptides Form Voltage-Dependent Ion-Permeable Channels in Planar Lipid Bilayer Membranes. *PNAS* **1990**, 210-214.

(55) Pazgier, M.; Wei, G.; Ericksen, B.; Jung, G.; Wu, Z.; de Leeuw, E.; Yuan, W.; Szmacinski, H.; Lu, W. Y.; Lubkowski, J.; Lehrer, R. I.; Lu, W. Sometimes It Takes Two to Tango: Contributions of Dimerization to Functions of Human α-Defensin HNP1 Peptide. *J. Biol. Chem.* **2012**, *287* (12), 8944–8953.

(56) Zhao, L.; Tolbert, W. D.; Ericksen, B.; Zhan, C.; Wu, X.; Yuan, W.; Li, X.; Pazgier, M.; Lu, W. Single, Double and Quadruple Alanine Substitutions at Oligomeric Interfaces Identify Hydrophobicity as the Key Determinant of Human Neutrophil Alpha Defensin HNP1 Function. *PLoS One.* **2013**, *8* (11).

(57) Ganz, T. Defensins: Antimicrobial Peptides of Innate Immunity. *Nat. Rev. Immunol.* **2003**, 710–720.

(58) Michael, E.; Selsted; Andre, J.; Ouellette. Defensins in granules of phagocytic and non-phagocytic cells. *Trends Cell Biol.* ***1995***, *5* (3), 114-119.

(59) Ganz, T.; Selsted, M. E.; Szklarek, D.; Harwig, S. S. L.; Daher, K.; Bainton, D. F.; Lehrer, R. I. Defensins Natural Peptide Antibiotics of Human Neutrophils. *J. Clin. Invest.* **1985**, *76* (4), 1427-1435.

(60) Hill, C.P.; Yee, J. Crystal Structure of Defensin HNP-3, an Amphiphilic Dimer Mechanisms of Membrane Permeabilization *Science* **1991**, *251* (5000), 1481-1481.

(61) Chan, D. I.; Prenner, E. J.; Vogel, H. J. Tryptophan- and Arginine-Rich Antimicrobial Peptides: Structures and Mechanisms of Action. *BBA-Biomembranes* **2006**, 1184–1202.

(62) Bonucci, A.; Balducci, E.; Pistolesi, S.; Pogni, R. The Defensin-Lipid Interaction: Insights on the Binding States of the Human Antimicrobial Peptide HNP-1 to Model Bacterial Membranes. *BBA-Biomembranes* **2013**, *1828* (2), 758–764.

(63) Nagaoka,I,; Hirota,S,; Yomogida,S.; Ohwada,A,; Hirata,M.; Synergistic actions of antibacterial neutrophil defensins and cathelicidins. *Inflamm. Res.* **2000**, *49* (2),73-79.

(64) Drab, E.; Sugihara, K. Cooperative Function of LL-37 and HNP1 Protects Mammalian Cell Membranes from Lysis. *Biophys. J.* **2020**, *119* (12), 2440–2450.

(65) Ebersberger, L.; Schindler, T.; Kirsch, S. A.; Pluhackova, K.; Schambony, A.; Seydel, T.; Böckmann, R. A.; Unruh, T. Lipid Dynamics in Membranes Slowed Down by Transmembrane Proteins. *Front. Cell. Dev. Biol.* **2020**, *8*.

(66) Soumpasis, D. M. Theoretical Analysis of Fluorescence Photobleaching Recovery Experiments. *Biophys. J.* **1983**, *41* (1), 95–97.

(67) Carnell, M.; Macmillan, A.; Whan, R. Fluorescence Recovery after Photobleaching (FRAP): Acquisition, Analysis, and Applications. *Methods Mol. Biol.* **2015**, *1232*, 255–271.

(68) Richter, R. P.; Bérat, R.; Brisson, A. R. Formation of Solid-Supported Lipid Bilayers: An Integrated View. *Langmuir* **2006**, *22* (8), 3497–3505.

(69) Granéli, A.; Rydström, J.; Kasemo, B.; Höök, F. Formation of Supported Lipid Bilayer Membranes on SiO2 from Proteoliposomes Containing Transmembrane Proteins. *Langmuir* **2003**, *19* (3), 842–850.

(70) Arouri, A.; Kiessling, V.; Tamm, L.; Dathe, M.; Blume, A. Morphological Changes Induced by the Action of Antimicrobial Peptides on Supported Lipid Bilayers. *J. Phys. Chem. B* **2011**, *115* (1), 158–167.

(71) Lopes, S.; Neves, C. S.; Eaton, P.; Gameiro, P. Cardiolipin, a Key Component to Mimic the E. Coli Bacterial Membrane in Model Systems Revealed by Dynamic Light Scattering and Steady-State Fluorescence Anisotropy. *Ana. Bioanal. Chem.* **2010**, 398, 1357–1366.

(72) Lind, T. K.; Wacklin, H.; Schiller, J.; Moulin, M.; Haertlein, M.; Pomorski, T. G.; Cárdenas, M. Formation and Characterization of Supported Lipid Bilayers Composed of Hydrogenated and Deuterated Escherichia Coli Lipids. *PLoS One* **2015**, *10* (12).

(73) Horne, J. E.; Brockwell, D. J.; Radford, S. E. Role of the Lipid Bilayer in Outer Membrane Protein Folding in Gram-Negative Bacteria. *J. Biol. Chem.* **2020**, 10340–10367.

(74) Weiskopf, D.; Schmitt, E. K.; Klühr, M. H.; Dertinger, S. K.; Steinem, C. Micro-BLMs on Highly Ordered Porous Silicon Substrates: Rupture Process and Lateral Mobility. *Langmuir* **2007**, *23* (18), 9134–9139.

(75) Sugihara, K.; Vörös, J.; Zambelli, T. A Gigaseal Obtained with a Self-Assembled Long-Lifetime Lipid Bilayer on a Single Polyelectrolyte Multilayer-Filled Nanopore. *ACS Nano* **2010**, *4* (9), 5047–5054.

(76) Tsemperouli, M.; Amstad, E.; Sakai, N.; Matile, S.; Sugihara, K. Black Lipid Membranes: Challenges in Simultaneous Quantitative Characterization by Electrophysiology and Fluorescence Microscopy. *Langmuir* **2019**, *35* (26), 8718–8757.

(77) Kalinowski, S.; Figaszewski, Z. A New System for Bilayer Lipid Membrane Capacitance Measurements: Method, Apparatus and Applications**.** *BBA-Biomembranes* **1992**, 1112. 57-66

(78) Klapper, Y.; Nienhaus, K.; Röcker, C.; Ulrich Nienhaus, G. Lipid Membranes and Single Ion Channel Recording for the Advanced Physics Laboratory. *Am. J. Phys.* **2014**, *82* (5), 502–509.

(79) Kalinowski, S.; Figaszewski, Z. A Four-Electrode System for Measurement of Bilayer Lipid Membrane Capacitance. *Meas. Sci. Technol.* **1995**, 6.

(80) Benz, R.; Frohlich, O.; uger, P. L.; Montal, M. Electrical Capacity of Black Lipid Films and of Lipid Bilayers Made from Monolayers. *BBA-Biomembranes* **1975,** 394, 323–334.

(81) Tsemperouli, M.; Sugihara, K. Characterization of Di-4-ANEPPS with Nano-Black Lipid Membranes. *Nanoscale* **2018**, *10* (3), 1090–1098.

(82) Karaballi, R. A. Spectroscopic Investigation of the Interaction between Biomimetic Membranes and Protein Aggregates. Saint Mary's University, **2015**.

(83) Sun, S.; Zhao, G.; Huang, Y.; Cai, M.; Shan, Y.; Wang, H.; Chen, Y. Specificity and Mechanism of Action of Alpha-Helical Membrane-Active Peptides Interacting with Model and Biological Membranes by Single-Molecule Force Spectroscopy. *Sci. Rep.* **2016**, *6*.

(84) Wang, B.; Zhang, J.; Zhang, Y.; Mao, Z.; Lu, N.; Liu, Q. H. The Penetration of a Charged Peptide across a Membrane under an External Electric Field: A Coarse-Grained Molecular Dynamics Simulation. *RSC Adv.* **2018**, *8* (72), 41517–41525.

(85) Wieprecht, T.; Seelig, J. Isothermal Titration Calorimetry for Studying Interactions between Peptides and Lipid Membranes. *Curr. Top. Membr.* **2002**, 31-56.

(86) Zhao, J.; Sugihara, K. Analysis of PDA Dose Curves for the Extraction of Antimicrobial Peptide Properties. *J. Phys Chem. B* **2021**, *125* (44), 12206–12213.

(87) Kim, J.; Mosior, M.; Chung, L. A.; Wu, H.; McLaughlin, S. Binding of Peptides with Basic Residues to Membranes Containing Acidic Phospholipids. *Biophys. J.* **1991**, *60* (1), 135–148.

(88) Burdach, K.; Tymecka, D.; Urban, A.; Lasek, R.; Bartosik, D.; Sek, S. Interactions of Linear Analogues of Battacin with Negatively Charged Lipid Membranes. *Membranes* **2021**, *11* (3).

(89) Scheinpflug, K.; Krylova, O.; Nikolenko, H.; Thurm, C.; Dathe, M. Evidence for a Novel Mechanism of Antimicrobial Action of a Cyclic R-,W-Rich Hexapeptide. *PLoS One* **2015**, *10* (4).

(90) Sautrey, G.; el Khoury, M.; Giro Dos Santos, A.; Zimmermann, L.; Deleu, M.; Lins, L.; Décout, J. L.; Mingeot-Leclercq, M. P. Negatively Charged Lipids as a Potential Target for New Amphiphilic Aminoglycoside Antibiotics: A Biophysical Study. *J. Biol. Chem.* **2016**, *291* (26), 13864–13874.

(91) Seelig, J. Thermodynamics of Lipid-Peptide Interactions. *BBA-Biomembranes* **2004**, 40–50.

(92) Chen, X.; Niyonsaba, F.; Ushio, H.; Okuda, D.; Nagaoka, I.; Ikeda, S.; Okumura, K.; Ogawa, H. Synergistic Effect of Antibacterial Agents Human β-Defensins, Cathelicidin LL-37 and Lysozyme against Staphylococcus Aureus and Escherichia Coli. *J. Dermatol. Sci.* **2005**, *40* (2), 123–132.

(93) Matsuzaki, K.; Mitani, Y.; Akada, K. Y.; Murase, O.; Yoneyama, S.; Zasloff, M.; Miyajima, K. Mechanism of Synergism between Antimicrobial Peptides Magainin 2 and PGLa. *Biochemistry* **1998**, *37* (43), 15144–15153.

(94) Zerweck, J.; Strandberg, E.; Bürck, J.; Reichert, J.; Wadhwani, P.; Kukharenko, O.; Ulrich, A. S. Homo- and Heteromeric Interaction Strengths of the Synergistic Antimicrobial Peptides PGLa and Magainin 2 in Membranes. *Eur. Biophys. J. Biophy.* **2016**, *45* (6), 535–547.

(95) Zerweck, J.; Strandberg, E.; Kukharenko, O.; Reichert, J.; Bürck, J.; Wadhwani, P.; Ulrich, A. S. Molecular Mechanism of Synergy between the Antimicrobial Peptides PGLa and Magainin 2. *Sci. Rep.* **2017**, *7* (1).

(96) Pardi A.; Zhang X L.; Selsted M E.; Skalicky J. J.; Yip F Ping. NMR studies defensin antimicrobial peptides. 2. Three-dimensional structures of rabbit NP-2 and human HNP-1. *Biochemistry* **1992**, *31* (46), 11357-11364.

(97) Xhindoli, D.; Pacor, S.; Guida, F.; Antcheva, N.; Tossi, A. Native Oligomerization Determines the

Mode of Action and Biological Activities of Human Cathelicidin LL-37. *Biochem. J.* **2014**, *457* (2), 263–275.

(98) Albani, J. R. Origin of Tryptophan Fluorescence Lifetimes Part 1. Fluorescence Lifetimes Origin of Tryptophan Free in Solution. *J. Fluoresc.* **2014**, *24* (1), 93–104.

(99) Ghisaidoobe, A. B. T.; Chung, S. J. Intrinsic Tryptophan Fluorescence in the Detection and Analysis of Proteins: A Focus on Förster Resonance Energy Transfer Techniques. *Int. J. Mol. Sci.* **2014**, 22518–22538.

(100) Bonucci, A.; Balducci, E.; Pistolesi, S.; Pogni, R. The Defensin-Lipid Interaction: Insights on the Binding States of the Human Antimicrobial Peptide HNP-1 to Model Bacterial Membranes. *Biochim. Biophys. Acta Biomembr.* **2013**, *1828* (2), 758–764.

(101) Ladokhin, A. S.; Jayasinghe, S.; White, S. H. How to Measure and Analyze Tryptophan Fluorescence in Membranes Properly, and Why Bother? *Anal. Biochem.* **2000**, *285* (2), 235–245.

(102) Sudheendra, U. S.; Dhople, V.; Datta, A.; Kar, R. K.; Shelburne, C. E.; Bhunia, A.; Ramamoorthy, A. Membrane Disruptive Antimicrobial Activities of Human β-Defensin-3 Analogs. *Eur. J. Med. Chem.* **2015**, 91, 91–99.

(103) Morgera, F.; Vaccari, L.; Antcheva, N.; Scaini, D.; Pacor, S.; Tossi, A. Primate Cathelicidin Orthologues Display Different Structures and Membrane Interactions. *Biocheml. J.* **2009**, *417* (3), 727–735.

(104) Morris, C. J.; Beck, K.; Fox, M. A.; Ulaeto, D.; Clark, G. C.; Gumbleton, M. Pegylation of Antimicrobial Peptides Maintains the Active Peptide Conformation, Model Membrane Interactions, and Antimicrobial Activity While Improving Lung Tissue Biocompatibility Following Airway Delivery. *Antimicrob. Agents Chemother.* **2012**, *56* (6), 3298–3308.

(105) Tossi, A.; Sandri, L.; Giangaspero, A. Amphipathic, α-Helical Antimicrobial Peptides. *Biopolymers* **2000**, *55* (1), 4–30.